

Black Holes: from Speculations to Observations

Thomas W. Baumgarte[†]

Department of Physics and Astronomy, Bowdoin College, Brunswick, ME 04011
Department of Physics, University of Illinois at Urbana-Champaign, Urbana, IL 61801

Abstract. This paper provides a brief review of the history of our understanding and knowledge of black holes. Starting with early speculations on “dark stars” I discuss the Schwarzschild “black hole” solution to Einstein’s field equations and the development of its interpretation from “physically meaningless” to describing the perhaps most exotic and yet “most perfect” macroscopic object in the universe. I describe different astrophysical black hole populations and discuss some of their observational evidence. Finally I close by speculating about future observations of black holes with the new generation of gravitational wave detectors.

THEORETICAL CONSIDERATIONS

This paper summarizes a talk presented at the Albert Einstein Century International Conference, held in Paris, France, in July 2005 to mark the centennial of Einstein’s “miracle” year 1905. Strictly speaking, black holes are a consequence of another Einstein miracle that did not occur in 1905 and still had to wait ten years, namely general relativity. With his theory of special relativity, however, Einstein had laid the ground work already in 1905 for his theory of general relativity. And even more strictly speaking, speculations on black holes predate even the special theory of relativity by over a century.

Early Speculations

In the late 1700’s John Mitchell [1] in England and Jean Simon Laplace [2] in France independently realized that celestial bodies that are both small and massive may become invisible¹. The basis for this speculation is the observation that the escape speed

$$v_{\text{esc}} = \sqrt{\frac{2GM}{R}}, \quad (1)$$

where M and R are the stellar mass and radius, is independent of the mass of the test particle. Within Newton’s particle theory of light it seems quite reasonable that this should also apply to light, in which case light can no longer escape the star if the escape speed exceeds the speed of light,

$$v_{\text{esc}} > c. \quad (2)$$

Evidently this happens when

$$GM > \frac{c^2 R}{2}, \quad (3)$$

meaning that stars with a large enough mass and a small enough radius become “dark”. Laplace went on to speculate that such objects may not only exist, but even in as great a number as the visible stars. With the demise of the particle theory of light, however, these speculations also lost popularity, and dark stars remained obscure until well after the development of general relativity.

¹ An excellent review of the history of our understanding of compact objects can be found in [3].

General Relativity and the Schwarzschild solution

In 1915 Albert Einstein published his field equations of general relativity [4],

$$G_{ab} = 8\pi G T_{ab}. \quad (4)$$

One could argue that superficially this equation may not be all that different from the Newtonian field equation

$$\nabla^2 \phi = 4\pi G \rho. \quad (5)$$

The left-hand-side of the Newtonian field equation (5) features a second derivative of the Newtonian potential ϕ , and the right-hand-side contains matter densities ρ . Quite similarly the Einstein tensor G_{ab} on the left-hand-side of Einstein's field equations (4) contains second derivatives of the fundamental object of general relativity, the spacetime metric g_{ab} . To complete the analogy, the stress-energy tensor T_{ab} on the right-hand-side contains matter sources. For the vacuum solutions in which we are interested in this article, the stress-energy tensor vanishes, $T_{ab} = 0$.

Unfortunately the Einstein tensor G_{ab} contains many lower-order, non-linear terms, making Einstein's equations a complicated set of ten coupled, quasi-linear equations for the ten independent components of the spacetime metric g_{ab} . Clearly, it is very difficult to find meaningful exact solutions. Karl Schwarzschild, returning fatally wounded from the battle fields of World War I, was nevertheless able to derive a fully non-linear solution in spherical symmetry within a year of Einstein's original publication [5]. Written as a line element ds^2 , the spacetime metric g_{ab} describing this solution is

$$ds^2 = g_{ab} dx^a dx^b = - \left(1 - \frac{G}{c^2} \frac{2M}{r} \right) dt^2 + \left(1 - \frac{G}{c^2} \frac{2M}{r} \right)^{-1} dr^2 + r^2 d\theta^2 + r^2 \sin^2 \theta d\phi^2. \quad (6)$$

This solution is the direct analog of the Newtonian point-mass solution

$$\phi = \frac{GM}{r} \quad (7)$$

and describes the strength of the gravitational fields, expressed by the spacetime metric g_{ab} , created by a point mass M at a distance r . The relativistic Schwarzschild solution (6) is significantly more mysterious than its Newtonian analog, though. Particularly puzzling is the "Schwarzschild radius"

$$r_s = \frac{2GM}{c^2} \quad (8)$$

at which the metric (6) becomes singular. The existence of this singularity obscured the physical interpretation of this solution, and in fact Schwarzschild himself died believing that his metric was physically irrelevant.

Other aspects also contributed to the fact that the astrophysical significance of the Schwarzschild solution (6) remained unappreciated for decades. For one thing it was not clear how such an object could possibly form, even though in 1939 Oppenheimer and Snyder [6] published a remarkable analytic calculation describing the "continued gravitational contraction" of a dust ball that leaves behind the Schwarzschild metric (6). This calculation, serving as a crude model of stellar collapse, made several simplifying assumptions: that the matter has zero pressure (so that it can be described as dust), that the angular momentum is zero, and that the spacetime is spherically symmetric. Critics maintained that in any realistic astrophysical situation none of these assumptions would hold, and that any deviation from these idealizations could easily halt the collapse, preventing continued gravitational contraction. The absence of angular momentum seems particularly troubling. Since the Schwarzschild solution does not carry any angular momentum it was completely unclear how any astrophysical object, which would necessarily carry *some* angular momentum, could collapse and form such a solution.

Finally, no astronomical observations had revealed phenomena requiring a gravitationally collapsed object as an explanation. Given that at least some of the astronomical community had been quite reluctant to accept the much less exotic White Dwarfs as an astrophysical reality, it is not surprising that a solution to Einstein's field equations that became singular at finite radius was not immediately embraced as a celestial object.

All three of these factors – a lack of understanding of the singularity at the Schwarzschild radius, general skepticism concerning gravitational collapse, and the absence of astronomical observations of gravitationally collapsed objects – resulted in the fact that the great astrophysical significance of Schwarzschild's solution (6) remained unappreciated for almost 50 years. All of this changed in the 1960's, the "golden age of black hole physics".

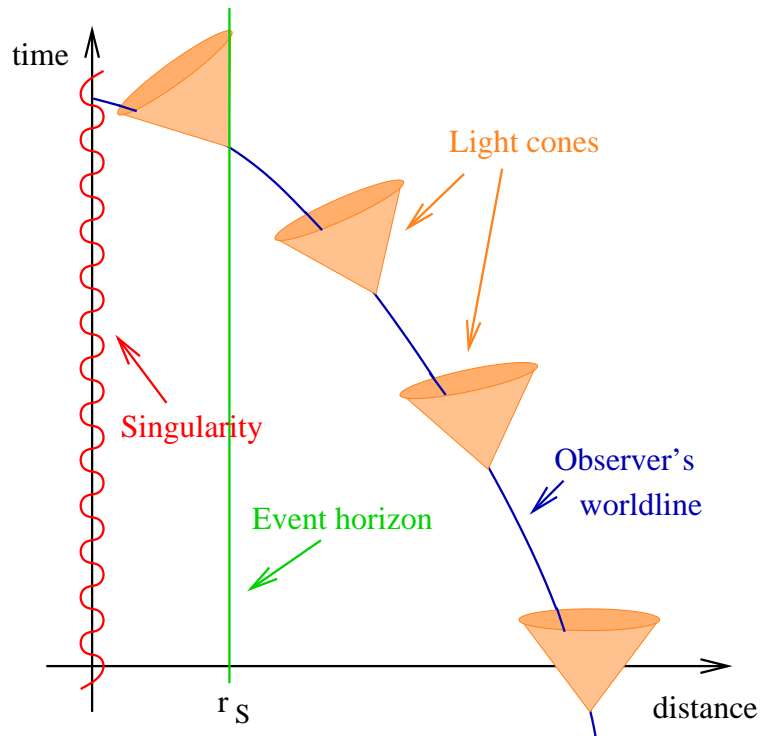


FIGURE 1. Cartoon of a spacetime singularity surrounded by an event horizon at $r_S = 2M$. The light cones of an observer falling into the black hole become increasingly tilted, until they completely tip over at the event horizon.

THE GOLDEN AGE OF BLACK HOLE PHYSICS

The golden age of black hole physics was ushered in when advances in our theoretical understanding of the Schwarzschild geometry and gravitational collapse in general coincided with new astronomical observations of highly energetic objects that clearly pointed to a gravitationally collapsed object as their central engine.

The Schwarzschild geometry

To begin with, it became clear that the apparent singularity at the Schwarzschild radius r_S (8) is simply a harmless coordinate singularity, not completely unlike the poles of a sphere when described in terms of longitude and latitude. This was demonstrated by Kruskal [7], who introduced a new coordinate system² that remains perfectly regular at r_S . Instead of being a mysterious singularity the Schwarzschild radius now emerged as a point of no return: a one-way membrane called “event horizon” through which nothing, not even light can leave the collapsed region inside. Inside this event horizon lurks a true singularity at which the curvature of spacetime becomes infinite³.

Consider the unfortunate observer in the spacetime cartoon of Figure 1. As long as he is far away from the event horizon an “outgoing” light ray emitted away from the horizon can propagate toward larger distance almost as easily as an “ingoing” ray emitted toward the horizon can propagate toward smaller distance. At this point the observer’s local light cone, which is the section of spacetime on which light propagates, is almost upright, and he can easily send signals to a buddy even further away. As our first observer approaches the event horizon, however, his light cones become increasingly tilted, and it becomes increasingly difficult for outgoing light rays to actually move outward. At

² Interesting, at least one other regular coordinate system had already been found by Painlevé [8] and Gullstrand [9]. Lemaître [10] similarly concluded that the geometry at the Schwarzschild radius must be regular, but apparently these conclusions remained unnoticed.

³ In a classical description of general relativity, that is. A self-consistent quantum theory of gravity will presumably resolve this singularity.

the event horizon the light cone tips over. An “outgoing” light ray emitted exactly on the event horizon will hover at the Schwarzschild radius forever, and inside this point all light rays, even “outgoing” ones, immediately move inward. Nothing can emerge from the event horizon and everything inside will soon reach the singularity that lurks at the black hole’s center. Our observer will cross the event horizon and reach the singularity in finite proper time. As seen by his buddy far away, his signals slowly fade away as he approaches the event horizon. Note also that the in-falling observer would not necessarily observe anything special occurring at the event horizon. Ultimately the observer will be torn apart by the increasingly strong tidal forces, but that may occur inside or outside the event horizon, depending on the black hole’s mass. It is only through careful experiments with flashlights, studying the properties of outgoing light-rays, that the observer would be able to tell that he has crossed an event horizon.

It is interesting to note that, by sheer coincidence, the location of the event horizon r_S (8) as expressed in Schwarzschild coordinates coincides exactly with the radius of a “dark star” (3) as determined by Mitchell and Laplace.

Gravitational Collapse

Almost simultaneously with the improved understanding of the Schwarzschild geometry, it became clear that gravitational collapse is much more generic than was believed earlier. In 1963 Roy Kerr [11] discovered a generalization of the Schwarzschild solution (6) that carries angular momentum. With this discovery the argument that objects carrying angular momentum cannot collapse gravitationally immediately collapsed itself. The first numerical relativity simulations also demonstrated that pressure may not be able to prevent gravitational collapse [12].

Further progress in our understanding of gravitational collapse arrived with a number of theorems. Perhaps most importantly Roger Penrose [13] showed that the formation of a spacetime singularity is generic after a so-called trapped surface has formed. Another set of theorems are collectively called the “no-hair” theorems⁴; in essence these theorems state that black holes have no distinguishing features. That is to say that Kerr’s solution describing a rotating black hole is the *only* solution describing a rotating black hole – all stationary black holes are Kerr black holes, parametrized only by their mass M and the angular momentum J ⁵. Black holes can be perturbed, but any perturbation is quickly radiated away, leaving behind a Kerr black hole.

This is a truly remarkable statement: it means that the structure of black holes is *uniquely* determined by their mass and angular momentum alone, completely independently of what formed the black hole at first place. This observation led Chandrasekhar to eloquently conclude in his Nobel Lecture

This is the only instance we have of an exact description of a macroscopic object... They are, thus, almost by definition, the most perfect macroscopic objects there are in the universe.

Observational Evidence

The technical advances during World War II lead to the development of radio astronomy in the post-war years. Within a few years several discrete sources had been detected, but with few exceptions the origin of these sources remained a mystery. It was generally believed that the sources were otherwise dark “radio stars” in our galaxy, since at extra-galactic distances they would have to be enormously energetic. This opinion started to change when the positioning of these “quasars” improved, and some were identified with galaxies.

The true breakthrough arrived when lunar occultations of the radio source 3C273 lead to its identification with another object whose optical spectrum showed a redshift of $z = 0.158$ – clearly establishing it as an extra-galactic object. This realization is documented in the remarkable March 16 issue of Nature [17, 18, 19, 20]. The same volume contains a theoretical paper by Hoyle and Fowler [21], in which the authors conclude⁶

Our present opinion is that only through the contraction of a mass of $10^7 - 10^8 M_\odot$ to the relativity limit can the energies of the strongest sources be obtained.

⁴ See, e.g., Israel [14], Carter [15], Robinson [16].

⁵ Strictly speaking black holes can also carry a charge Q , but from an astrophysical perspective this is irrelevant since any charge would very be neutralized very quickly.

⁶ See also Ginzburg [22].

These events ushered in “Relativistic Astrophysics” as a new field. As a sign of the time the first *Texas Symposium on Relativistic Astrophysics* was convened in December of 1963. The new field also attracted many new people into the field, including John Wheeler. In fact, it was John Wheeler who in 1967 coined the term *black hole*, marking the transition from speculative ideas on dark stars to the astrophysical reality of black holes⁷.

ASTROPHYSICAL BLACK HOLES

Clearly, we do not have any absolutely water-tight proof that black holes exist in our universe. However, we do have some extremely convincing evidence that makes black holes by far the most conservative explanation of the observed phenomena.

Observations clearly point to two different populations of black holes. One of these populations are “stellar-mass black holes”, which have masses in the order of $10 M_{\odot}$; another group are “supermassive black holes”, which have masses in the order of $10^6 - 10^9 M_{\odot}$. I will discuss these two groups in more detail below. There is also some observational evidence for “intermediate mass black holes” of about $10^3 - 10^4 M_{\odot}$, and finally there are speculations on “primordial black holes” that would be left over from the big bang. Even though these different kinds of black holes have vastly different masses, they are, from a mathematical perspective, the exact same kind of animal: a Kerr solution to Einstein’s field equations with certain values for their mass and angular momentum. From an astrophysical perspective they differ not only in their mass and angular momentum, but also in how we can observe them and in how they form, i.e. in their evolutionary history.

Stellar-mass black holes: Cygnus X-1

The prime example of a stellar-mass black hole is Cygnus X-1⁸, which was first discovered in the data of the X-ray satellite Uhuru, launched on Dec 12 1970. The case for Cygnus X-1 as a black hole can be summarized as follows⁹: To begin with, Cygnus X-1 shows very short time variations in the X-ray signal (in the order of $\Delta t \sim 10$ ms and less). This implies that Cyg X-1 is a very small object, in the order of $R \lesssim c\Delta t \lesssim 10^6$ m. It is also the unseen binary companion to a 9th magnitude supergiant star called HDE226868. The Doppler curve of this star shows that the binary has an orbital period of about 5.6 days; from the amplitude of the Dopplershift we can determine the mass function f to be about $0.25M_{\odot}$ [25]. Combining this with the mass of supergiant stars we can derive a lower limit on the mass of Cyg X-1,

$$M_{\text{Cyg X-1}} \gtrsim 3.3M_{\odot}. \tag{9}$$

An independent argument involving some constraints on the binary’s orbit arrives at a similar limit.

Given its size, Cyg X-1 has to be a “compact object”: a white dwarf, a neutron star, or a black hole. Even under very conservative assumptions both white dwarfs and neutron stars have maximum masses safely below the lower limit of Cyg X-1’s mass. This leaves a black hole as the most likely explanation.

Cyg X-1 is an example of a *stellar-mass* black hole, which form the end-point of the evolutionary cycle for massive stars. When massive stars run out of nuclear fuel they can no longer support themselves against gravitational contraction. For stars with masses larger than about $20 M_{\odot}$ nothing can halt the subsequent gravitational collapse, which therefore leads to prompt black hole formation. For stars with masses between about 8 and $20 M_{\odot}$ the collapse can be halted when the density of the compressed stellar material reaches nuclear densities. The resulting shock-wave launches a “core-collapse” supernova and leaves behind a newly formed neutron star. This neutron star may either remain stable, or it may form a black hole at a later time. A “delayed collapse” to a black hole can be triggered by a variety of mechanisms, including fall-back of matter and phase transitions in the neutron star interior. Finally, two neutron stars may collide. If the remnant exceeds the maximum allowed mass for rotating neutron stars this coalescence will also lead to the formation of a stellar-mass black hole¹⁰.

⁷ I again refer to Israel [3] for a much more complete account of the developments described in this Section.

⁸ See Oda [23] for a review and references.

⁹ See Section 13.5 and Box 13.1 in Shapiro and Teukolsky [24] for a detailed discussion.

¹⁰ Even if the remnant exceeds the maximum allowed mass for *uniformly* rotating neutron stars it may be stabilized temporarily by virtue of *differential* rotation [26]. Dissipation of the differential rotation, for example by magnetic coupling, then triggers a delayed collapse

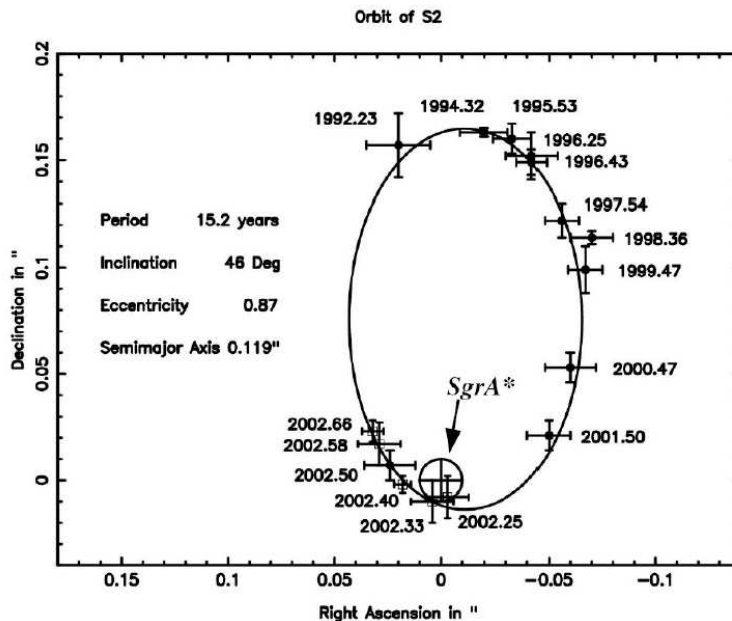


FIGURE 2. Orbit of the star S2 around SgrA* (Figure from [28]).

We currently know of about 20 confirmed black hole binaries¹¹, but presumably that is only a tiny fraction of the total number of stellar-mass black holes in our own galaxy.

Supermassive black holes: Sagittarius A*

Perhaps the most convincing evidence for a black hole comes from the center of our own galaxy, Sagittarius A* [28, 29]. Observations of our galactic center in the near infrared reveal several stars that orbit a central object in bound orbits¹². Particularly compelling is the orbit of the star S2, about two-thirds of which has now been mapped with increasingly accurate positioning (see Figure 2). The emerging orbit is a Kepler orbit with a period P of about 15 years and a semi-major axis a of about 4.62 mpc. From Kepler's third law we can conclude that the enclosed mass is

$$M = \frac{4\pi^2 a^3}{GP^2} \approx 4 \times 10^6 M_{\odot} \quad (10)$$

S2's orbit also has a significant eccentricity of $e = 0.87$. At pericenter its distance to the central object is only 124 AU. This implies that the central object harbors an enormous mass in a very small volume. The most conservative explanation for such an object – which also must have remained stable over the lifetime of the galaxy – is again a black hole.

Sagittarius A* is an example of a *supermassive* black hole. There is some very convincing evidence for supermassive black holes in other galaxies as well – for example the maser observations from NGC 4258 (also known as M106) [30]. In fact, there is evidence that supermassive black holes lurk at the cores of most galaxies [31].

It is less clear exactly how supermassive black holes form. Many different routes may lead to the formation of massive black holes in active galactic nuclei¹³, but which of these routes nature tends to take is still under debate. A constraint comes from the recent observation of quasars at redshift $z \approx 6$ in the Sloan Digital Sky Survey [33]. If these quasars are indeed powered by supermassive black holes, this implies that the latter must have formed very quickly in

¹¹ See Table 4.1 in McClintock and Remillard [27].

¹² A beautiful movie animation of these orbits can be found at www.mpe.mpg.de/ir/GC.

¹³ See, e.g., the flow chart in Fig. 1 of [32].

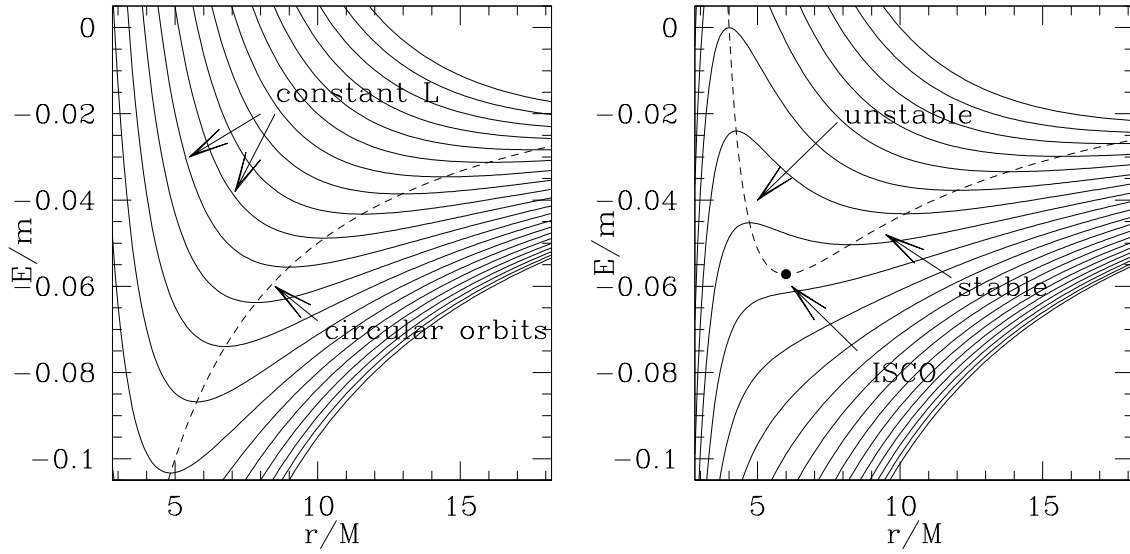


FIGURE 3. The binding energy E/mc^2 as a function of separation rc^2/GM of a test mass m in orbit about a Newtonian point mass M (left panel) and a Schwarzschild black hole of mass M (right panel). The solid lines denote contours of constant orbital angular momentum L . Extrema of these contours identify circular orbits, marked by the dashed lines. The circular orbits are stable if the extremum is a minimum, otherwise they are unstable.

the early universe. One model that may account for that is accretion onto seed black holes that form in the collapse of first-generation (Pop. III) stars [34, 35].

Probing black hole properties

Most observational evidence for black holes to date is based on the argument “a lot of mass in a tiny volume”, which leaves black holes as the most conservative explanation. Also, most observations to date only provide information about the black hole mass, and not about the angular momentum. Clearly it would be desirable to go beyond that.

A number of efforts are under way to find observational evidence for certain black hole characteristics. One such characteristic is the absence of a stellar surface. X-rays emitted by black hole candidates indeed shows some differences from that emitted by neutron stars. These differences can be explained in terms of an accretion flow hitting the stellar surface in the case of neutron stars, but freely falling through the horizon in case of the black holes¹⁴. Another effort aims at resolving the event horizon of Sgr A*, which would show up as a “black hole shadow” since it absorbs all radiation emitted behind it.

An interesting idea for the measurement of the black hole angular momentum J is based on the concept of the *Innermost Stable Circular Orbit*, or ISCO for short. Consider a test mass m in orbit about a point mass M . A circular orbit can be found by identifying an extremum of the test mass’s binding energy E at constant orbital angular momentum L ; a minimum corresponds to a stable circular orbit, while a maximum corresponds to an unstable orbit.

In Newtonian physics the binding energy as a function of separation r is given by

$$\frac{E}{mc^2} = -\frac{GM}{c^2 r} + c^2 \frac{\tilde{L}^2}{2r^2}, \quad (11)$$

where $\tilde{L} = L/mc^2$. To find an extremum of the binding energy we differentiate with respect to r at constant \tilde{L} and set the result to zero,

$$\tilde{L}^2 = \frac{GM}{c^4} r, \quad (12)$$

¹⁴ See Najayan [36] for a review and references.

which we recognize as Kepler's third law (since $\tilde{L} = \Omega r^2/c^2$). Evidently we can find a circular orbit for arbitrary r , and the equilibrium energy of these circular orbits results from inserting (12) back into (11),

$$E_{\text{bind}} = \frac{1}{2} \frac{GMm}{r}. \quad (13)$$

We can also verify that all these extrema are minima, meaning that the orbits are stable. Alternatively, we can identify the orbits graphically as in the left panel in Fig. 3.

For a test mass in orbit about a Schwarzschild black hole the binding energy is given by

$$\frac{E}{mc^2} = \left(\left(1 - \frac{G}{c^2} \frac{2M}{r} \right) \left(1 + c^2 \frac{\tilde{L}^2}{r^2} \right) \right)^{1/2} - 1, \quad (14)$$

where r is the Schwarzschild radius. Taking derivatives we would find that circular orbits exist only for radii $r > 3GM/c^2$. Moreover, these orbits are stable only outside

$$r_{\text{ISCO}} = \frac{6GM}{c^2}, \quad (15)$$

which therefore marks the ISCO for a test particle orbiting a Schwarzschild black hole (see also the right panel in Fig. 3).

The presence of an ISCO is of great relevance for black hole observations because most of the emitted radiation is believed to originate from an accretion disk. In this accretion disk particles follow almost circular orbits as they spiral toward the black hole. Since circular orbits are unstable inside the ISCO, the accretion disk can only exist outside r_{ISCO} . Accordingly, the Doppler shift of spectral lines is limited by the speed of matter at the ISCO. The key point is that the location of the ISCO depends on the black hole's angular momentum J ; it is at $r_{\text{ISCO}} = 6GM/c^2$ only for a Schwarzschild black hole with $J = 0$, and can get much closer to the event horizon for a spinning Kerr black hole. For a spinning black hole the accretion disk may therefore extend closer to event horizon, and the correspondingly higher speeds result in a greater broadening of the emitted spectral lines. Some results based on this idea have been reported in [37].

Even if successful, however, these techniques can only determine the global parameters M and J . Clearly it would be desirable to map out the local properties of the spacetime geometry around a black hole. Our best chance of doing that comes with gravitational wave observations.

GRAVITATIONAL RADIATION

Sources of gravitational radiation

Maxwell's equations predict that accelerating charges emit electromagnetic radiation. For an electric dipole, the emitted power is given by the Lamor formula

$$L_{\text{em}} = \frac{2}{3c^3} \ddot{d}_i \ddot{d}_i, \quad (16)$$

where d_i is the electric dipole moment, \ddot{d}_i its second time derivative, and where we sum over repeated indices.

Einstein's equations similarly predict that accelerating masses emit gravitational radiation. One might expect that the power emitted from a gravitational wave source is given by an expression similar to Lamor's formula. However, the analog of the electric dipole moment is the mass dipole moment, and its first time derivative the total momentum. For an isolated system the total momentum is constant, so that the second derivative of the dipole moment vanishes – there is no gravitational dipole radiation. The first – and often dominant – contribution to gravitational radiation comes from the quadrupole term. The equivalent of the Lamor formula in general relativity is therefore

$$L_{\text{GW}} = \frac{1}{5} \frac{G}{c^5} \langle \ddot{\mathcal{I}}_{jk} \ddot{\mathcal{I}}_{jk} \rangle \quad (17)$$

Here \mathcal{I}_{ij} is the reduced quadrupole moment

$$\mathcal{I}_{jk} = \int \rho \left(x_j x_k - \frac{1}{3} \delta_{jk} r^2 \right) d^3x = \sum_A m_A \left(x_j x_k - \frac{1}{3} \delta_{jk} r^2 \right), \quad (18)$$

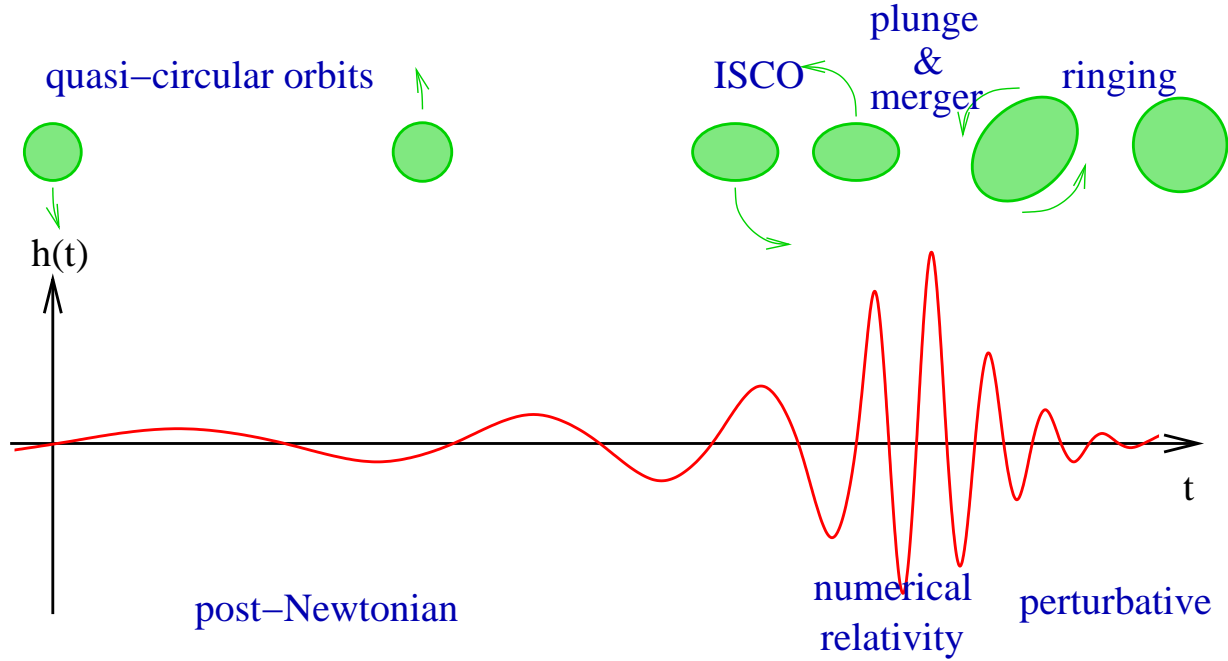


FIGURE 4. Cartoon describing the inspiral of a black hole binary.

the bracket $\langle \rangle$ denotes averaging over several characteristic periods of the system, and the triple dot denotes the third time derivative. For a strong signal of gravitational radiation we evidently need large and rapidly changing quadrupole moments, which brings to mind binary systems.

To estimate L_{GW} for a binary system we evaluate \mathcal{I}_{jk} for a Newtonian binary and find

$$L_{\text{GW}} = \frac{32}{5} \frac{G^4}{c^5} \frac{M^3 \mu^2}{a^5}. \quad (19)$$

Here $M = m_1 + m_2$ is the binary's total mass, $\mu = m_1 m_2 / M$ the reduced mass and a the semi-major axis, and we have also used Kepler's law to eliminate the orbital frequency Ω . Inserting numbers we find that the only binary systems that emit appreciable amounts of gravitational radiation have huge masses and very small binary separations a . The most promising candidates are therefore *compact binaries* consisting of black holes or neutron stars.

The loss of energy due to the emission of gravitational radiation leads a shrinking of the binary's orbit. To see this we compute

$$\frac{da}{dt} = \frac{dE/dt}{dE/da} = -\frac{L_{\text{GW}}}{dE_{\text{bind}}/da} = -\frac{64}{5} \left(\frac{G}{c^2} \frac{M^{2/3} \mu^{1/3}}{a} \right)^3 c, \quad (20)$$

where

$$E_{\text{bind}} = \frac{1}{2} \frac{GM\mu}{a} \quad (21)$$

is the generalization of (13). Computing the loss of angular momentum we would also find that the emission of gravitational radiation leads to a reduction of the binary's eccentricity, i.e. to a circularization of its orbit.

A binary inspiral then proceeds as illustrated in Fig. 4. Presumably the binary starts out at a large binary separation. The emission of gravitational radiation leads to a continuous decrease in the binary separation, and also to a decrease in the binary's eccentricity. At sufficiently late times we may therefore approximate the binary orbit as circular, except for the slow inspiral. As the binary separation shrinks, both the amplitude and the frequency of the emitted gravitational wave signal increases. This leads to the typical "chirp" signal sketched in Fig. 4. In analogy to our discussion of point masses orbiting a single black hole, the binary will at some point reach an ISCO. Inside this separation it is energetically favorable for the binary companions to abandon circular orbits, and instead plunge toward each other

and merge. In the final “ring-down” phase the remnant will settle down quickly into an axisymmetric equilibrium object.

Even for the most promising sources of gravitational radiation any astrophysical signal that we might hope for is going to be extremely weak. To see this we estimate the effect of a gravitational wave on the spacetime metric g_{ab} . If the spacetime is almost flat, we may write $g_{ab} = \eta_{ab} + h_{ab}$, where η_{ab} is the flat Minkowski metric and where h_{ab} is the small perturbation that we observe as a gravitational wave. For a perturbation caused by a distant gravitational wave source we have

$$h_{ij}^{\text{TT}} = \frac{2}{s} \frac{G}{c^4} \mathcal{J}_{ij}^{\text{TT}} \left(t - \frac{s}{c} \right). \quad (22)$$

Here the symbol TT denotes the “transverse traceless” part of the corresponding tensors, s is the distance from the observer to the gravitational wave source, and the quadrupole moment \mathcal{J}_{ij} is evaluated at the retarded time $t - s/c$. We again evaluate this term for a Newtonian binary, and estimate the gravitational wave amplitude to be in the order of

$$h \approx \frac{1}{s} \frac{G}{c^4} M a^2 \Omega^2 \approx \frac{G^2}{c^4} \frac{M}{s} \frac{M}{a} \approx \frac{r_s}{s} \frac{r_s}{a}, \quad (23)$$

where we have used Kepler’s third law to eliminate Ω and where r_s is the Schwarzschild radius (8) of the mass M . Evidently we expect the strongest gravitational wave signal h_{ij} when the binary’s semi-major axis a is small, i.e. close to the ISCO where $a \approx r_s$ (if we neglect factors of a few).

Consider, for example, a stellar-mass compact binary that is coalescing somewhere in the Virgo cluster. For such a binary, r_s is in the order of a few km, and the distance s is about 15 Mpc or a few 10^{20} km. We then have $h \approx 10^{-20}$. Since the corrections h_{ij} are added to the background metric, which is of order unity, the relative change in the spacetime metric is exceedingly small, and the proposal to measure these perturbations remarkably ambitious.

The weakness of any gravitational wave signal that we may realistically expect has two important consequences for the prospect of observing them: we need extremely sensitive gravitational wave detectors, and we need accurate models of any potential sources to aid in the identification of any signal in the noisy output of the detector. We will discuss both of these aspects in the following two Sections.

Gravitational wave detectors

A new generation of gravitational wave observatories is now operational. Basically, these instruments are gigantic Michelson-Morley interferometers. The two LIGO observatories in the US, for example, have an arm-length of 4 km. Somewhat smaller instruments exist in Italy (VIRGO), Germany (GEO), and Japan (TAMA), and another observatory is currently under construction in Australia (ACIGA). The idea is that a gravitational wave h_{ij} passing through these interferometers will slightly distort the relative length of the two perpendicular arms. Tracking these distortions with the help of laser interferences as a function of time should reveal the passing gravitational wave signal.

The ground-based detectors mentioned above all have arm-lengths in the order of a kilometer, which makes them sensitive to the gravitational radiation emitted from stellar-mass black holes¹⁵. A space-based gravitational wave antenna LISA with an arm-length of several million kilometer is being planned; this instrument would be sensitive to gravitational radiation emitted from supermassive black holes.

As we have seen in the previous section an astrophysical gravitational wave signal that we might realistically expect will lead to a tiny perturbation of the spacetime metric and hence to only a minuscule distortion in the arm-lengths of the interferometers – in fact, only a tiny fraction of the size of the nucleus of a hydrogen atom. It is therefore extremely difficult to reduce the dominant sources of noise – seismic, thermal and photon shot-noise – and increase the signal-to-noise ratio so that an astrophysical source can be identified unambiguously.

It is therefore truly remarkable that the LIGO collaboration has recently achieved its design goal of a strain sensitivity exceeding 10^{-22} for a large part of its frequency range (see Fig. 5). Given this sensitivity, and assuming a signal-to-noise ratio of eight, LIGO is now able to detect binary neutron stars to a distance somewhat greater than 10 Mpc. For binary black holes with a slightly larger mass this range is also slightly larger, and already includes the Virgo cluster.

Whether or not the current LIGO observatory, LIGO I, will be able to detect a binary black hole system – or any other source of gravitational radiation – depends on how often such binaries coalesce in our or our neighboring galaxies.

¹⁵ In geometric units a solar mass equals 1.48 km.

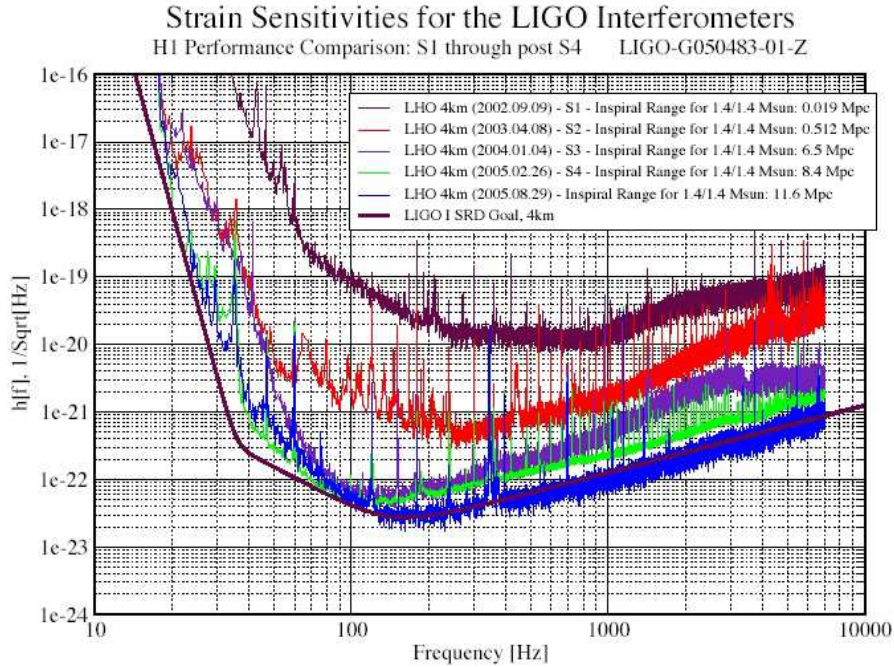


FIGURE 5. Strain sensitivities for the LIGO Hanford (Washington) interferometer (Figure courtesy the LIGO Scientific Collaboration).

Estimates for binary neutron star systems can be based on the statistics of known binaries¹⁶, while estimates for binary black hole systems, which have never been observed, are typically based on population synthesis calculations¹⁷. According to these estimates it is not completely impossible that LIGO I will observe a compact binary, and it seems almost certain that an advanced LIGO II observatory, as it is currently being planned, will see many such sources.

We finally point out that a gravitational wave detector tracks the amplitude of a gravitational wave at one particular point in space, but, unlike a telescope, does not produce an image. A single detector therefore cannot position any source. Two detectors can position a source to a ring in the sky, and with the world-wide network of detectors there is hope that any potential source can be positioned to within a reasonable accuracy.

Source modeling

Different approximations can be used to model the inspiral of a compact binary in its different phases. For the initial inspiral, while the binary separation is sufficiently large and the effects of relativistic and tidal interactions sufficiently small, post-Newtonian point-mass calculations provide excellent approximations¹⁸. The very late stage can be modeled very accurately with the help of perturbation theory¹⁹. Neither one of these approximations can be used in the intermediate regime around the ISCO during which the binary emits the strongest gravitational wave signal. The most promising tool for the modeling of this dynamical phase of the binary coalescence and merger is numerical relativity²⁰.

¹⁶ See, e.g. [38, 39].

¹⁷ For example [40].

¹⁸ See, e.g., [41], as well as L. Blanchet's article in this volume.

¹⁹ E.g. [42].

²⁰ See [43] for a recent review.

Numerical relativity calculations typically adopt a 3+1 decomposition. In such a decomposition the four-dimensional space M is carved up into a foliation of three-dimensional spatial slices Σ , each one of which corresponds to an instant of constant coordinate time t . Einstein equations for the four-dimensional spacetime metric g_{ab} can then be rewritten as a set of three-dimensional equations for the three-dimensional, spatial metric γ_{ij} on the spatial slices Σ , as well as its time derivative.

The general coordinate freedom of general relativity has an important consequence for the structure of these three-dimensional equations. Since there are three space coordinates and one time coordinate, we can choose four of the ten independent components of the symmetric spacetime metric g_{ab} freely. But that means that the ten equations in Einstein’s equations (4) cannot be independent – otherwise the metric would be over-determined. Four of the ten equations in Einstein’s equations must be redundant. In the framework of a 3+1 decomposition these four equations are *constraint equations* that constrain the gravitational fields within each spatial slice Σ , while the remaining six *evolution equations* govern the time-evolution of γ_{ij} from one slice Σ to the next. The equations are compatible, meaning that fields that satisfy the constraint equations at one instant of time continue to satisfy the constraints at all later times if the fields are evolved with the evolution equations. This structure of the equations is very similar to that of Maxwell’s equations, where the “div” equations constrain the electric and magnetic field at any instant of time, while the “curl” equations govern the dynamical evolution of the fields.

Finding a numerical solution to Einstein’s equations usually proceeds in two steps. In the first step the constraint equations are solved to construct *initial data*, describing the gravitational fields together with any matter or other sources at some initial time, and in the second step these data are *evolved* forward in time by solving the evolution equations.

One of the challenges in constructing initial data results from the fact that the constraint equations determine only some of the gravitational fields. The remaining fields are related to the degrees of freedom associated with gravitational waves, which depend on the past history and cannot be determined from Einstein’s equations at only one instant of time. Instead, these “background fields” are freely specifiable and have to be chosen before the constraint equations can be solved. The challenge, then, lies in making appropriate choices that reflect the astrophysical scenario one wishes to model.

For the modeling of binary black holes we would like to construct initial data that model a binary at a reasonably close binary separation outside the ISCO as it emerges from the inspiral from a much larger separation. We expect such a binary to be in “quasi-equilibrium”, meaning that the orbit is circular (except for the slow inspiral) and that the individual black holes are in equilibrium. A number of different approaches have been pursued, but currently the best approximations to quasi-equilibrium black holes are the models of Cook and Pfeiffer [44]. Probably there are ways to improve these data, in particular as far as the background fields and the resulting “gravitational wave content” are concerned²¹, but even without these improvements the current models are probably excellent approximations.

While initial data describing binary black holes have been reasonably well understood for a number of years, progress on dynamical simulations of black holes has been much slower. Until recently, these simulations had been plagued by numerical instabilities that made the codes crash long before the black holes had done anything interesting. The past year, however, has seen a dramatic break-through in this field, and by now several groups can perform reliable simulations of the binary black hole coalescence, merger and ring-down.

The first announcement of such a calculation came from Pretorius [48]. His approach differs from the more traditional numerical relativity calculations in that he integrates the four-dimensional Einstein equations (4) directly, instead of casting them into a 3+1 form²². The left panel of Fig. 6 shows a gravitational wave form from one of his recent simulations, starting with the initial data of [44]. At early times some noise is seen, which is either related to the imperfect initial data themselves or the imperfect matching of the numerical methods used in the initial data and the evolution. The noise disappears quickly, and leaves behind a very clean waveform, tracking the inspiral through several orbits, through the plunge and merger, until the newly formed remnant settles down into a single Kerr black hole.

Shortly after Pretorius’ announcement a number of other groups announced similarly successful calculations [51, 52, 53]. All of these later simulations do adopt a 3+1 decomposition of Einstein’s equations, and cast these equations in the BSSN form [54, 55]. The right panel of Fig. 6 shows the trajectory of the black holes in the calculation of Campanelli et al. [47]. Campanelli et al. [51, 47] and Baker et al. [52] adopt a particularly simple method that treats

²¹ One approach is to match the background fields to the post-Newtonian approximation of the prior inspiral [45]; another promising suggestion is a “wave-less” approximation proposed by Shibata et al. [46].

²² The equations are expressed in a way, however, that leads to particularly desirable mathematical properties; see [49, 50].

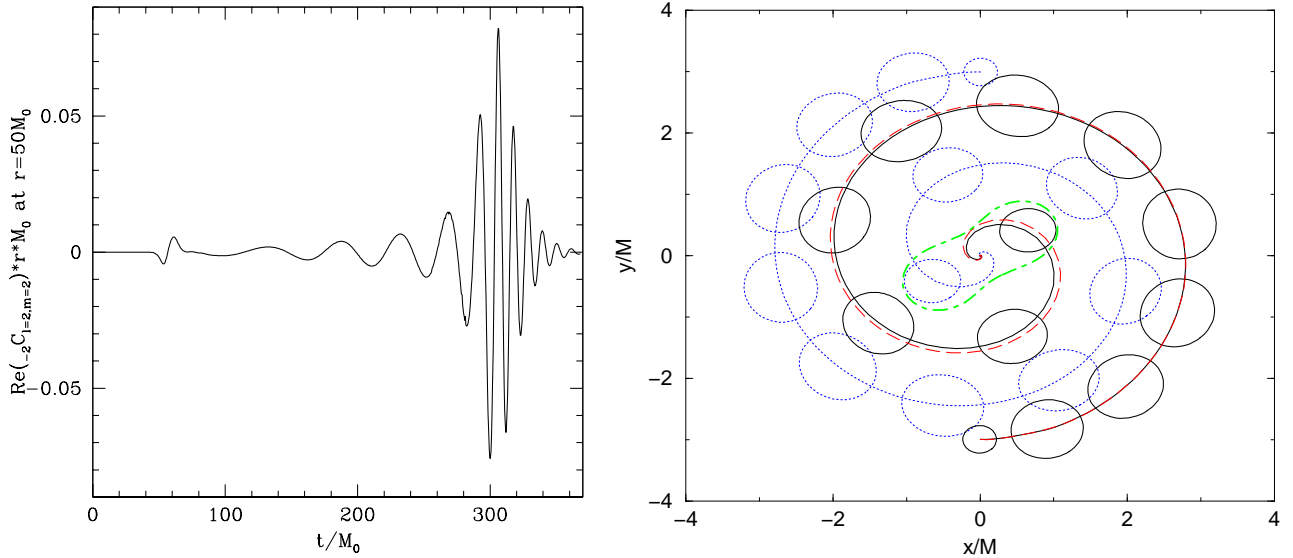


FIGURE 6. The left panel shows the gravitational wave form $\text{Re}(\psi_4)$ from a binary black hole coalescence as recently computed by Pretorius (private communication). The right panel shows the trajectory of the black hole horizons in the calculation of Campanelli et al. [47].

the black hole singularities as “punctures” and avoids having to excise the black hole interior from the numerical grid [56, 57]. In the meantime several follow-ups on these calculations have already been published, including simulations of binaries with mass-ratios different from unity [58, 59] and spinning black holes [60].

Especially comparing with the situation just a year ago, it is truly remarkable and reassuring that different groups using independent techniques and implementations can now carry out reliable simulations of binary black hole coalescence and merger. It may still be a while until results from these simulations can be used to assemble a catalog of realistic wave templates to be used in the analysis of data from gravitational wave detectors, but the past year has certainly seen a huge step forward in that direction.

SUMMARY

Black holes may well be the most fascinating consequence of Einstein’s theory of general relativity. Similarly fascinating is the development of our understanding of black holes. Speculations on so-called “dark stars” actually predate both special and general relativity by over a century, but it nevertheless took almost half a century after the publication of general relativity and Schwarzschild’s derivation of his famous solution until black holes became generally accepted as an astrophysical reality.

By now we have very convincing observational evidence for both stellar-mass and supermassive black holes. So far these observations only constrain the black hole mass, and clearly it would be desirable to probe the local black hole geometry in addition to the global parameters. There is hope that we will be able to do that in the near future with the new generation of gravitational wave detectors. The LIGO observatories have recently achieved their design sensitivities, enabling us to detect inspiraling binary black holes to a distance of approximately the Virgo Cluster. The next generation Advanced LIGO will improve the sensitivity by over a factor of ten, which increases the event rate by over a factor of thousand. With the recent advances in numerical relativity we are also much closer to producing theoretical gravitational wave templates, which will aid both in the identification of gravitational wave signals and in their interpretation. There is hope, then, that we can discuss detailed gravitational wave observations of binary black holes by the time we celebrate the centennial of Einstein’s general relativity.

ACKNOWLEDGMENTS

It is a pleasure to thank Karen A. Topp for a careful reading of this manuscript. This article was supported in part by NSF Grant PHY-0456917 to Bowdoin College.

REFERENCES

1. J. Mitchell, *Phil. Trans. R. Soc. Lond.* **141**, 1232 (1796).
2. P. S. Laplace, *Exposition du systeme du monde*, L'imprimerie du Cercle-Social, Paris, l'an IV de la République Française (otherwise known as 1795).
3. W. Israel, "Dark stars: the evolution of an idea," in *300 years of gravitation*, edited by S. Hawking, and W. Israel, Cambridge University Press, Cambridge, 1973.
4. A. Einstein, *Sitzungsberichte the Preussischen Akademie der Wissenschaften* pp. 844–847 (1915).
5. K. Schwarzschild, *Sitzungsberichte the Deutschen Akademie der Wissenschaften* pp. 189–196 (1916).
6. K. Oppenheimer, and H. Snyder, *Phys. Rev.* **56**, 455 (1939).
7. M. D. Kruskal, *Phys. Rev.* **119**, 1743 (1960).
8. P. Painlevé, *C. R. Acad. Sci. (Paris)* **173**, 677 (1921).
9. A. Gullstrand, *Arkiv Mat. Astron. Fys.* **16**, 1 (1922).
10. G. Lemaître, *Ann. Soc. Sci. (Bruxelles) A* **53**, 51 (1933).
11. R. P. Kerr, *Phys. Rev. Lett.* **11**, 237 (1963).
12. M. W. May, and R. H. White, *Phys. Rev.* **74**, 35 (1966).
13. R. Penrose, *Phys. Rev. Lett.* **14**, 57 (1965).
14. W. Israel, *Phys. Rev.* **164**, 1776 (1967).
15. B. Carter, *Phys. Rev. Lett.* **26**, 331 (1971).
16. D. C. Robinson, *Phys. Rev. Lett.* **34**, 905 (1975).
17. C. Hazard, M. B. Mackey, and A. J. Shimmins, *Nature* **197**, 1037 (1963).
18. M. Schmidt, *Nature* **197**, 1040 (1963).
19. J. B. Oke, *Nature* **197**, 1040 (1963).
20. J. Greenstein, and T. A. Matthews, *Nature* **197**, 1041 (1963).
21. F. Hoyle, and W. A. Fowler, *Nature* **197**, 533 (1963).
22. V. L. Ginzburg, *Sov. Astron.* **5**, 282 (1961).
23. M. Oda, *Space Sci. Rev.* **20**, 757 (1977).
24. S. L. Shapiro, and S. A. Teukolsky, *Black Holes, White Dwarfs and Neutron Stars: The Physics of Compact Objects*, Wiley-Interscience, New York, 1983.
25. D. R. Gies, and C. T. Bolton, *Astrophys. J.* **260**, 240 (1982).
26. T. W. Baumgarte, S. L. Shapiro, and M. Shibata, *Astrophys. J. Lett.* **528**, L29 (2000).
27. J. E. McClintock, and R. A. Remillard, "Black hole binaries," in *Compact Stellar X-ray Sources*, edited by W. H. G. Lewin, and M. van der Klis, Cambridge University Press, Cambridge, 2006.
28. R. Schödel, T. Ott, R. Genzel, R. Hofmann, M. Lehnert, A. Eckart, N. Mouawad, T. Alexander, M. J. Reid, R. Lenzen, M. Hartung, F. Lacombe, D. Rouan, E. Gendron, G. Rousset, A.-M. Lagrange, W. Brandner, N. Ageorges, C. Lidman, A. F. M. Moorwood, J. Spyromilio, N. Hubin, and K. M. Menten, *Nature* **419**, 694 (2002).
29. A. M. Ghez, G. Duchêne, K. Matthews, S. D. Hornstein, A. Tanner, J. Larkin, M. Morris, E. E. Becklin, S. Salim, T. Kremenek, D. Thompson, B. T. Soifer, G. Neugebauer, and I. McLean, *Astrophys. J. Lett.* **586**, L127 (2003).
30. M. Miyoshi, J. Moran, J. Herrnstein, L. Greenhill, N. Nakai, P. Diamond, and M. Inoue, *Nature* **373**, 127 (1995).
31. D. Richstone, E. A. Ajhar, R. Bender, G. Bower, A. Dressler, S. M. Faber, A. V. Filippenko, K. Gebhardt, R. Green, L. C. Ho, J. Kormendy, T. R. Lauer, J. Magorrian, and S. Tremaine, *Nature* **395**, A14 (1998).
32. M. Rees, *Ann. Rev. Astr. & Ap.* **22**, 471 (1984).
33. X. Fan, M. A. Strauss, D. P. Schneider, R. H. Becker, R. L. White, Z. Haiman, M. Gregg, L. Pentericci, E. K. Grebel, V. K. Narayanan, Y.-S. Loh, G. T. Richards, J. E. Gunn, R. H. Lupton, G. R. Knapp, Ž. Ivezić, W. N. Brandt, M. Collinge, L. Hao, D. Harbeck, F. Prada, J. Schaye, I. Strateva, N. Zakamska, S. Anderson, J. Brinkmann, N. A. Bahcall, D. Q. Lamb, S. Okamura, A. Szalay, and D. G. York, *Astron. J.* **125**, 1649 (2003).
34. S. L. Shapiro, *Astrophys. J.* **620**, 59 (2005).
35. M. Volonteri, and M. Rees, *Astrophys. J.* **633**, 624 (2005).
36. R. Najayan, *New J. Phys.* **7**, 199 (2005).
37. J. M. Miller, A. C. Fabian, C. S. Reynolds, M. A. Nowak, J. Homan, M. J. Freyberg, M. Ehle, T. Belloni, R. Wijnands, M. van der Klis, P. A. Charles, and W. H. G. Lewin, *Astrophys. J. Lett.* **606**, L131 (2004).
38. C. Kim, V. Kalogera, D. R. Lorimer, M. Ihm, and K. Belczynski, "The Galactic Double-Neutron-Star Merger Rate: Most Current Estimates," in *ASP Conf. Ser. 328: Binary Radio Pulsars*, edited by F. A. Rasio, and I. H. Stairs, 2005, p. 83.
39. V. Kalogera, C. Kim, D. R. Lorimer, M. Burgay, N. D'Amico, A. Possenti, R. N. Manchester, A. G. Lyne, B. C. Joshi, M. A. McLaughlin, M. Kramer, J. M. Sarkissian, and F. Camilo, *Astrophys. J. Lett.* **601**, L179 (2004).
40. R. Voss, and T. M. Tauris, *Mon. Not. Roy Astron. Soc.* **342**, 1169 (2003).

41. L. Blanchet, *Living Rev. Relativity* **5**, 3 (2002).
42. J. Baker, B. Brügmann, M. Campanelli, C. O. Lousto, and R. Takahashi, *Phys. Rev. Lett.* **87**, 121103 (2001).
43. T. W. Baumgarte, and S. L. Shapiro, *Phys. Rept.* **376**, 41 (2003).
44. G. B. Cook, and H. P. Pfeiffer, *Phys. Rev. D* **70**, 104016 (2004).
45. W. Tichy, B. Brügmann, M. Campanelli, and P. Diener, *Phys. Rev. D* **67**, 064008 (2003).
46. M. Shibata, K. Uryū, and J. L. Friedman, *Phys. Rev. D* **70**, 044044 (2004).
47. M. Campanelli, C. O. Lousto, and Y. Zlochower, *Phys. Rev. D* **73**, 061501 (2006).
48. F. Pretorius, *Phys. Rev. Lett.* **95**, 121101 (2005).
49. H. Friedrich, *Commun. Math. Phys.* **100**, 525 (1985).
50. D. Garfinkle, *Phys. Rev. D* **65**, 044029 (2002).
51. M. Campanelli, C. O. Lousto, P. Marronetti, and Y. Zlochower (2005), [gr-qc/0511048](#).
52. J. G. Baker, J. Centrella, C. Dai-II, M. Koppitz, and J. R. van Meter (2005), [gr-qc/0511103](#).
53. P. Diener, F. Herrmann, D. Pollney, E. Schnetter, E. Seidel, R. Takahashi, J. Thornburg, and J. Ventrella (2005), [gr-qc/0512108](#).
54. M. Shibata, and T. Nakamura, *Phys. Rev. D* **52**, 5428 (1995).
55. T. W. Baumgarte, and S. L. Shapiro, *Phys. Rev. D* **59**, 024007 (1999).
56. S. Brandt, and B. Brügmann, *Phys. Rev. Lett.* **78**, 3606 (1997).
57. T. W. Baumgarte, *Phys. Rev. D* **62**, 024018 (2000).
58. F. Herrmann, D. Shoemaker, and P. Laguna (2006), [gr-qc/0601026](#).
59. J. G. Baker, J. Centrella, C. Dai-II, M. Koppitz, J. R. van Meter, and M. C. Miller (2006), [astro-ph/0603204](#).
60. M. Campanelli, C. O. Lousto, and Y. Zlochower (2006), [gr-qc/0604012](#).